Figure S1

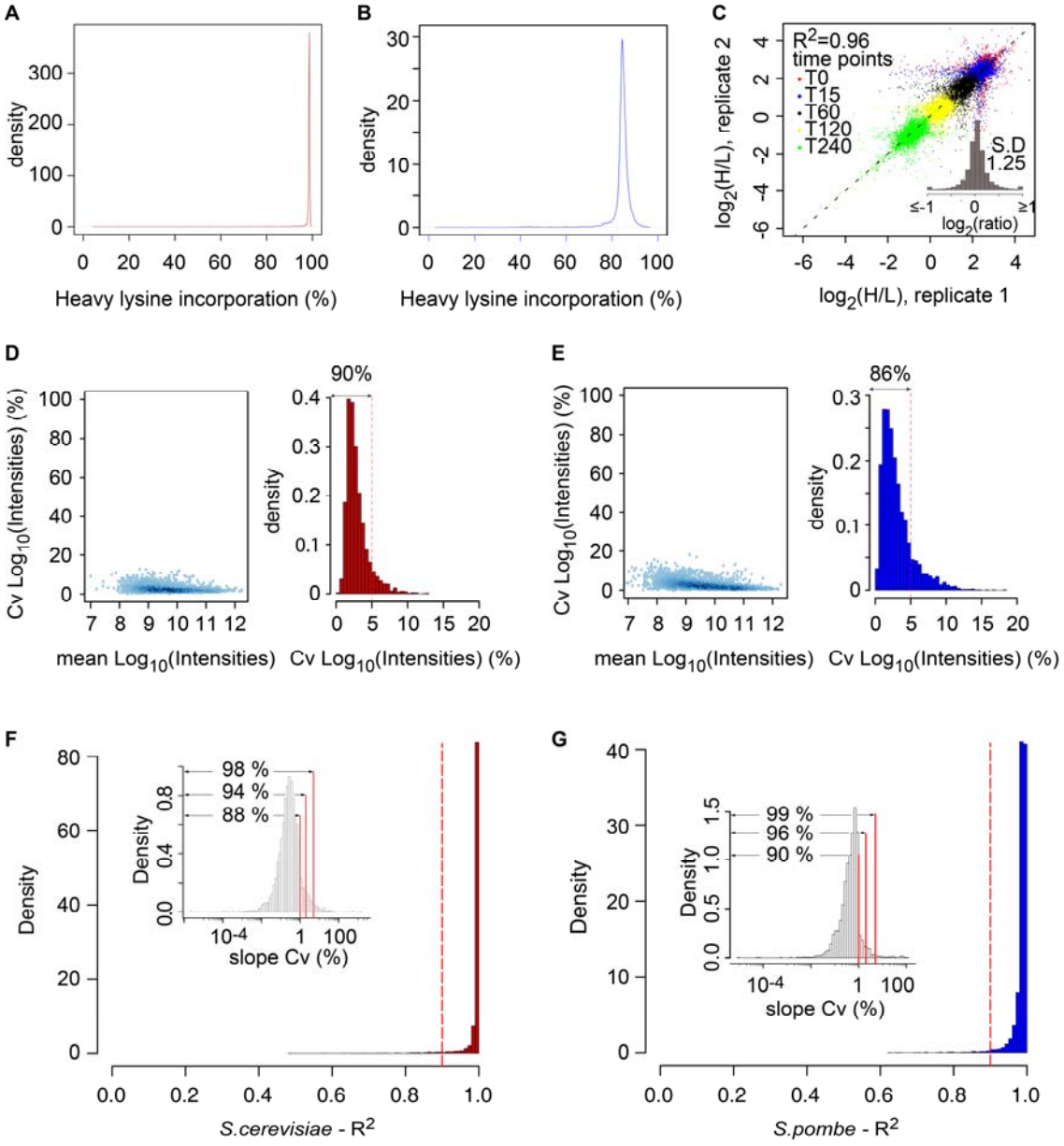
A
density
Heavy lysine incorporation (%)
B
density
Heavy lysine incorporation (%)
C
R2=0.96
time points
T0
T15
T60
T120
T240
S.D
1.25
log2(ratio)
log2(H/L), replicate 2
log2(H/L), replicate 1
D
Cv Log10(Intensities) (%)
mean Log10(Intensities)
90%
density
Cv Log10(Intensities) (%)
E
Cv Log10(Intensities) (%)
mean Log10(Intensities)
86%
density
Cv Log10(Intensities) (%)
F
Density
98 %
94 %
88 %
slope Cv (%)
S.cerevisiae - R2
G
Density
99 %
96 %
90 %
slope Cv (%)
S.pombe - R2

Figure S1, related to Figure 1: Quality of MS data (Incorporation of heavy lysine in yeasts, reproducibility of biological replicates in S. *pombe* and steady state of proteins) and quality of curve fitting to determine protein half-lives.

(A) Density function of the rates of heavy lysine incorporation of all lysine-containing peptides (98.9%) in *S. cerevisiae*. **(B)** Density function of the rates of heavy lysine incorporation of all lysine-containing peptides in *S. pombe* (84.4%). **(C)** Log_2 transformed "heavy" to "light" ratios of intensities from 49,541 unique peptides (log_2(H/L)) measured in the time course in two replicates. The insert shows the histogram of the log_2-transformed ratios (mean = 0.067, SD =1.25 expressed as a fold-change from the mean). (**D**) Protein steady state assumption in *S. cerevisiae*. Coefficient of variation of the log_{10} transformed protein intensity across the 6 time points. Histogram of the coefficient of variation of the log_{10} transformed protein abundances across the six times (mean = 2.9%, 90% less than 5% variation). (**E**) Protein steady state assumption in *S. pombe*. Coefficient of variation of the log_{10} transformed protein intensity across the 5 time points. Histogram of the coefficient of variation of the log_{10} transformed protein abundances across the six times (mean = 2.9%, 86% less than 5% variation). **(F)** Distribution of the goodness-of-fit of linear regression for 3,772 proteins in *S. cerevisiae* (3,676 proteins with $R^2 \geq 0.9$). Variability of linear regression slopes assed by leave-one-out cross validation (Cv) on the 3,676 proteins with $R^2 \geq 0.9$ (3,642, 88%, proteins with Cv≤0.1). **(G)** Distribution of the goodness-of-fit of linear regression for 3,075 proteins in *S. pombe* (3,025 proteins with $R^2 \geq 0.9$). Variability of linear regression slopes assed by leave-one-out cross validation (Cv) for the 3,025 proteins with $R^2 \geq 0.9$ (3,000, 90%, proteins with Cv≤0.1).

Figure S2

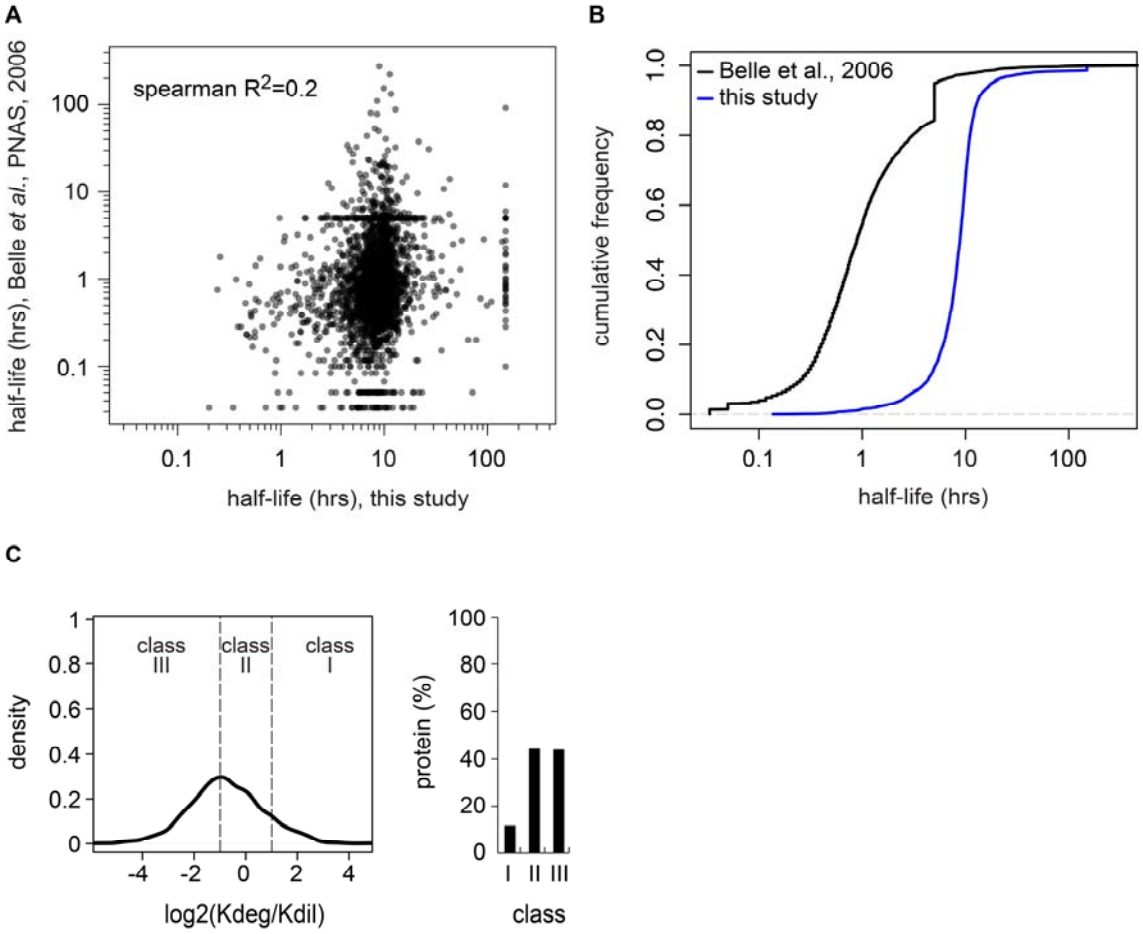
A
spearman R2=0.2
half-life (hrs), Belle et al., PNAS, 2006
half-life (hrs), this study
B
Belle et al., 2006
this study
cumulative frequency
half-life (hrs)
C
class III
class II
class I
density
log2(Kdeg/Kdil)
protein (%)
class

Figure S2, related to Figure 2. Comparison with half-lives determined by quantitation of degradation of TAP-tagged protein by western blot combined with cycloheximide treatment.

(A) Protein half-lives determined by pulse SILAC (this study) compared to protein half-lives determined by western blot quantitation combined with cycloheximide treatment of TAP-tagged proteins (Belle et al., 2006). **(B)** Cumulative frequency of protein half-lives determined by pulse SILAC (blue line, this study) and of protein half-lives determined by western blot quantitation combined with cycloheximide treatment of TAP-tagged proteins (Belle et al., 2006). **(C)** Contributions of degradation (Kdeg) and protein dilution due to cell growth (Kdil) in mouse fibroblasts NIH3T3 cells (Schwanhausser et al., 2011). Log2(Kdeg/Kdil) ratios define three classes of protein abundance regulation: class I (Kdeg ≥ 2xKdil), class II (0.5xKdil ≤ Kdeg ≥ 2xKdil) and class III (Kdeg ≤ 2xKdil).

Figure S3

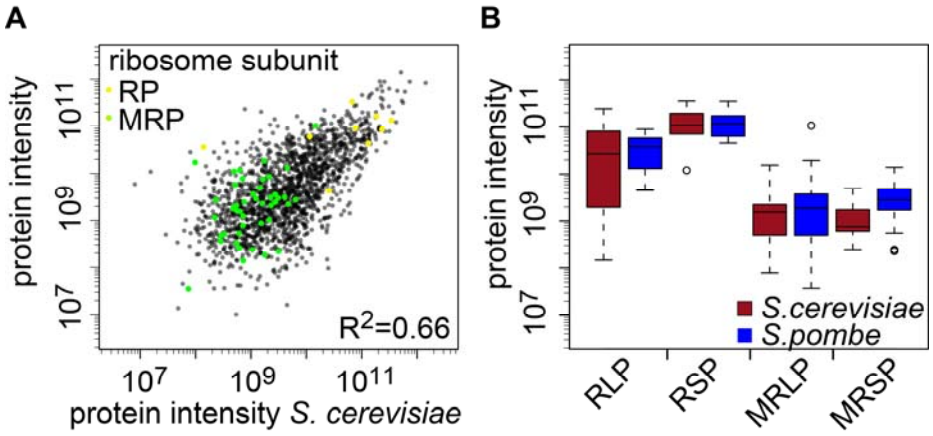
A
ribosome subunit
RP
MRP
protein intensity
10^7
10^9
10^{11}
R^2=0.66
protein intensity *S. cerevisiae*
B
protein intensity
10^7
10^9
10^{11}
S.cerevisiae
S.pombe
RLP
RSP
MRLP
MRSP

Figure S3, related to Figure 3. Abundance of ribosomal proteins and arginine biosynthetic process in *S. cerevisiae* and *S. pombe.*

(A) Abundances of ribosomal (RP, yellow dots) and mitochondrial ribosomal proteins (MRP, green dots) in *S. cerevisiae* compared to their counterpart abundances in *S. pombe*. **(B)** Boxplot of abundances of ribosomal large (RLP), ribosomal small (RSP), mitochondrial ribosomal large (MRLP) and mitochondrial ribosomal small proteins (MRSP) in *S. cerevisiae* and *S. pombe.*

Figure S4

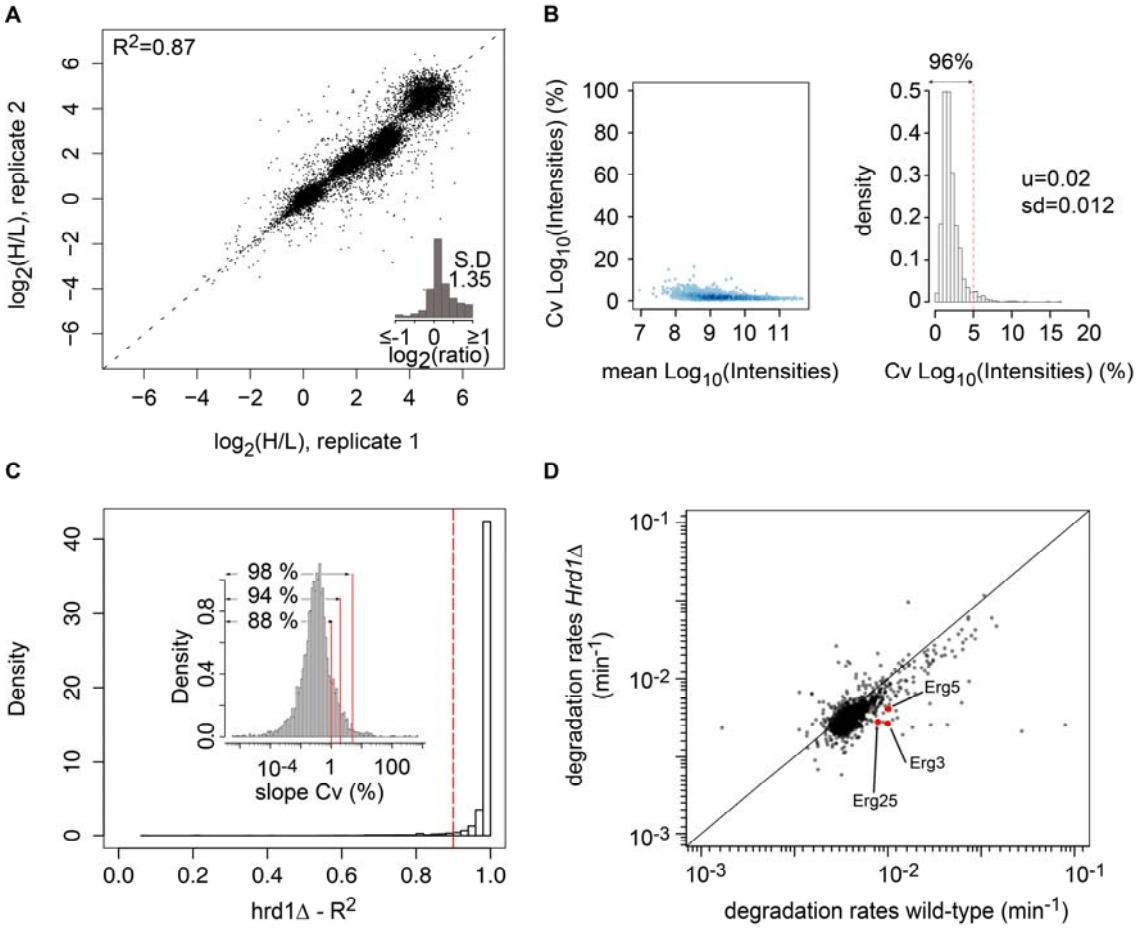
A
R2=0.87
log2(H/L), replicate 2
log2(H/L), replicate 1
S.D
1.35
≤-1 0 ≥1
log2(ratio)
B
Cv Log10(Intensities) (%)
mean Log10(Intensities)
96%
density
u=0.02
sd=0.012
Cv Log10(Intensities) (%)
C
Density
hrd1Δ - R2
98 %
94 %
88 %
slope Cv (%)
D
degradation rates Hrd1Δ (min-1)
degradation rates wild-type (min-1)
Erg5
Erg3
Erg25

Figure S4, related to Figure 4. Reproducibility of biological replicates, steady state of proteins abundances, quality of curve fitting to determine protein half-lives in *Hrd1*Δ cells and comparison of non-corrected degradation rates in wild-type versus *Hrd1*Δ cells.

A) Log_2 transformed "heavy" to "light" ratios of intensities from 23,561 unique peptides (log_2(H/L)) measured in the time course in two replicates. The insert shows the histogram of the log_2-transformed ratios (mean = 0.2, SD =1.35 expressed as a fold-change from the mean). **(B)** Protein steady state assumption in *S. cerevisiae*. Coefficient of variation of the log_{10} transformed protein intensity across the six times. Histogram of the coefficient of variation of the log_{10} transformed protein abundances across the four times (mean = 2.0%, 96% less than 5% variation). **(C)** Distribution of the goodness-of-fit of linear regression for 3,436 proteins in *S. cerevisiae hrd1*Δ (3,312 proteins with $R^2 \geq 0.9$). Variability of linear regression slopes assed by leave-one-out cross validation (Cv) for the 3,312 proteins with $R^2 \geq 0.9$ (3,280 proteins with Cv≤0.1). **(D)** Scatter plot of non-corrected degradation rates (min^{-1}) in wild-type versus *hrd1*Δ cells. Ergosterol enzymes in *hrd1*Δ cells are highlighted in red.

Table S1, related to Figure 1. Protein Half-lives in S. cerevisiae.

This table contains the degradation rates (min-1), the quality of the curve fitting (R2), the protein half-lives in minutes and hours and the analysis of the slope variability analyzed by leave-one-out cross validation determined in S. cerevisiae**.**

Table S2, related to Figure 1. Protein Half-lives in S. pombe.

This table contains the degradation rates (min-1), the quality of the curve fitting (R2), the protein half-lives in minutes and hours and the analysis of the slope variability analyzed by leave-one-out cross validation determined in S. pombe**.**

Table S3, related to Figure 2: Agreement between proteins half-lives reported in the literature and protein half-lives in this study.

Protein names	$T_{1/2}$ in literature (reference)	$T_{1/2}$ in the current study
Ste3	20 min (Gammie et al., 1995)	41.6min
Matalpha2	~5 min (Xie et al., 2010)	15.5 min
Chs2	~ 25 min (Chuang and Schekman, 1996)	44.4 min
Chs3	> 120 min (Chuang and Schekman, 1996)	222 min
Erg1	<120 min (Foresti et al., 2013)	83.2 min
Pho8	Between 6.4 and 9.9 hours (Qiao et al., 2009)	8.8 hours
Hxt6/7	~ 45 min (Krampe et al., 1998)	75.6 min
Tat1	>> 3hours (Suzuki et al., 2013)	4.6 hours
Tat2	~30 min (Hiraki and Abe, 2010)	~1 hour
Bap2	~ 60 min (Omura et al., 2001)	51 min

Table S4, related to Figure 2: classification of protein half-lives in S. *cerevisiae*, S. *pombe*, and NIH3T3.

	Description	S. *cerevisiae* (hrs)	S. *pombe* (hrs)
class I	short-lived proteins	≤ 1.25	≤ 2
class II	medium-lived proteins	[1.25;5]	[2;8]
class III	long-lived proteins	> 5	> 8

Table S5, related to Figure 4: Protein stabilized in *hrd1*Δ cells.

#	Gene names	Fold Change degradation rates (wild-type / Hrd1D)
1	TAP42	17.58
2	RGD1	11.27
3	RIM101	4.11
4	ORC1	3.54
5	VIK1	3.35
6	CWP1	2.83
7	GRS1	2.77
8	CMC1	2.74
9	RME1	2.42
10	CBP2	2.35
11	RAD9	2.01
12	TPO1	1.94
13	ERG3	1.94
14	RPO41	1.81
15	FET3	1.79
16	COS8	1.77
17	ATC1	1.76
18	DMA1	1.74
19	NSG2	1.74
20	ATG26	1.72
21	YDL156W	1.71
22	ADK2	1.69
23	FPS1	1.69
24	ERG25	1.67
25	YOR052C	1.65
26	GEP4	1.65
27	TY1B-ER1	1.65
28	MMR1	1.63
29	RGA1	1.63
30	NCE103	1.63
31	MSH1	1.62
32	RCY1	1.60
33	SLM2	1.59
34	SWC7	1.59
35	CIS3	1.59
36	SCM3	1.58
37	ERG5	1.57
38	TY1B-PR2	1.57
39	CCW14	1.55

40	CRH1	1.55
41	INM2	1.54
42	IRA1	1.53
43	YIL055C	1.53
44	YOR093C	1.53
45	ASH1	1.52
46	TFC8	1.51
47	MRL1	1.50
48	RTN2	1.49
49	BNA7	1.49
50	PSR1	1.49

Supplemental Experimental Procedures

Protein abundance fold change analysis by SILAC

Protein abundances fold-changes between BY4742 wild-type and the isogenic *hrd1*Δ strain were performed in biological duplicate following the protocol described in (Frohlich et al., 2013).

Sample preparation

For each time point, ~25 OD units of cells were harvested by centrifugation. Cells were lysed in 200 µl buffer containing 50 mM Tris/HCl pH=9.0, 5% SDS and 100 mM DTT for 30 min at 55°C. Lysates were cleared by centrifugation at 17000g for 10 min. Supernatants were diluted with buffer UA (8 M urea, 0.1 M Tris/HCl pH=8.5) to a final concentration of 0.5% SDS. Proteins were digested with the endoproteinase LysC following the protocol for filter-aided sample preparation (FASP, 12). Briefly, protein extracts were loaded on a 30k centricon filter unit (Amicon) by centrifugation at 14000g. Samples were washed twice by addition of 200 µl buffer UA and alkylated for 20 min in the dark by addition of 5.5 mM iodoacetamide (IAA) in 200 µl buffer UA. Samples were washed additional 4 times by addition of 200 µl buffer UA and centrifugation. 60 µl of buffer UA containing 0.5 mg/ml LysC were added to the filter units and incubated at 37°C over-night. Peptides were recovered by centrifugation into a fresh tube and additional elution with 200 µl of 0.5 M NaCl. Samples were acidified by addition of trifluoroacidic acid (TFA) and cleared of precipitates by centrifugation at 17000g for 5 min. Peptide concentration was measured and 5 µg of peptides were desalted following the protocol for StageTip purification 13. Samples were eluted with 60 µL buffer B (80% ACN, 0.1% formic acid in H20) and reduced in a Vacufuge plus (Eppendorf) to a final volume of 3 µL. 2 µL of buffer A (0.1 % formic acid in H_20) were added and the resulting 5 µL were injected into the HPLC.

Chromatography and Mass Spectrometry

Reversed phase chromatography was performed on a Thermo Easy nLC 1000 system connected to a Q Exactive mass spectrometer (Thermo) through a nano-electrospray ion source. Peptides were separated on 50-cm columns (New

Objective) with an inner diameter of 75 µm packed in house with 1.9 µm C18 resin (Dr. Maisch GmbH). Peptides were eluted from 50-cm columns with a linear gradient of acetonitrile from 5-27% in 0.1% formic acid for 240 min at a constant flow rate of 250 nl/min. The column temperature was kept at 40°C by an oven (Sonation GmbH, Germany) with a Peltier element. Eluted peptides from the column were directly electrosprayed into the mass spectrometer. Mass spectra were acquired on the Q Exactive in a data dependent-mode to automatically switch between full scan MS and up to 10 data dependent MS/MS scans. The maximum injection time for full scans was 20 ms with a target value of 3,000,000 at a resolution of 70,000 at m/z=200. The 10 most intense multiple charged ions (z≥2) from the survey scan were selected with an isolation width of 3Th and fragment with higher energy collision dissociation (HCD 14) with normalized collision energies of 25. Target values for MS/MS were set to 100,000 with a maximum injection time of 120 ms at a resolution of 17,500 at m/z=200. To avoid repetitive sequencing, the dynamic exclusion of sequenced peptides was set to 45 sec.

Data analysis

The resulting MS and MS/MS spectra were analyzed using MaxQuant (version 1.3.0.5), utilizing its integrated ANDROMEDA search algorithms. Peak lists were searched against the UNIPROT databases for S.cerevisiae or S.pombe with common contaminants added. The search included carbamidomethylation of cysteines as fixed modification, and methionine oxidation and N-terminal acetylation as variable modifications. Maximum allowed mass deviation for MS peaks was set to 6ppm and 20ppm for MS/MS peaks. Maximum missed cleavages were 3. The false discovery rate was determined by searching a reverse database. Maximum false-discovery rates were 0.01 both on peptide and protein levels. Minimum required peptide length was 6 residues. Proteins with at least two peptides (one of them unique) were considered identified. The “match between runs” option was enabled with a time window of 1 min to match identification between replicates.

Sequence analysis

The 30-mer upstream of the start codon of the 10% most abundant protein were subjected to logo analysis using the plogo website (https://plogo.uconn.edu/) (O'Shea et al., 2013) The 30-mer, upstream of the start codon in the 5′UTR, of all ORFs corresponding to the proteins present in the UNIPROT databases for *S. cerevisiae* were used as a background.

Supplemental references

Belle, A., Tanay, A., Bitincka, L., Shamir, R., and O'Shea, E.K. (2006). Quantification of protein half-lives in the budding yeast proteome. Proceedings of the National Academy of Sciences of the United States of America *103*, 13004-13009.

Chuang, J.S., and Schekman, R.W. (1996). Differential trafficking and timed localization of two chitin synthase proteins, Chs2p and Chs3p. The Journal of cell biology *135*, 597-610.

Foresti, O., Ruggiano, A., Hannibal-Bach, H.K., Ejsing, C.S., and Carvalho, P. (2013). Sterol homeostasis requires regulated degradation of squalene monooxygenase by the ubiquitin ligase Doa10/Teb4. eLife *2*, e00953.

Frohlich, F., Christiano, R., and Walther, T.C. (2013). Native SILAC: metabolic labeling of proteins in prototroph microorganisms based on lysine synthesis regulation. Molecular & cellular proteomics : MCP *12*, 1995-2005.

Gammie, A.E., Kurihara, L.J., Vallee, R.B., and Rose, M.D. (1995). DNM1, a dynamin-related gene, participates in endosomal trafficking in yeast. The Journal of cell biology *130*, 553-566.

Hiraki, T., and Abe, F. (2010). Overexpression of Sna3 stabilizes tryptophan permease Tat2, potentially competing for the WW domain of Rsp5 ubiquitin ligase with its binding protein Bul1. FEBS letters *584*, 55-60.

Krampe, S., Stamm, O., Hollenberg, C.P., and Boles, E. (1998). Catabolite inactivation of the high-affinity hexose transporters Hxt6 and Hxt7 of Saccharomyces cerevisiae occurs in the vacuole after internalization by endocytosis. FEBS letters *441*, 343-347.

O'Shea, J.P., Chou, M.F., Quader, S.A., Ryan, J.K., Church, G.M., and Schwartz, D. (2013). pLogo: a probabilistic approach to visualizing sequence motifs. Nature methods *10*, 1211-1212.

Omura, F., Kodama, Y., and Ashikari, T. (2001). The basal turnover of yeast branched-chain amino acid permease Bap2p requires its C-terminal tail. FEMS microbiology letters *194*, 207-214.

Qiao, W., Ellis, C., Steffen, J., Wu, C.Y., and Eide, D.J. (2009). Zinc status and vacuolar zinc transporters control alkaline phosphatase accumulation and activity in Saccharomyces cerevisiae. Molecular microbiology *72*, 320-334.

Schwanhausser, B., Busse, D., Li, N., Dittmar, G., Schuchhardt, J., Wolf, J., Chen, W., and Selbach, M. (2011). Global quantification of mammalian gene expression control. Nature *473*, 337-342.

Suzuki, A., Mochizuki, T., Uemura, S., Hiraki, T., and Abe, F. (2013). Pressure-induced endocytic degradation of the Saccharomyces cerevisiae low-affinity tryptophan permease Tat1 is mediated by Rsp5 ubiquitin ligase and functionally redundant PPxY motif proteins. Eukaryotic cell *12*, 990-997.

Xie, Y., Rubenstein, E.M., Matt, T., and Hochstrasser, M. (2010). SUMO-independent in vivo activity of a SUMO-targeted ubiquitin ligase toward a short-lived transcription factor. Genes & development *24*, 893-903.